

Cluster-Based Beaconing Process For VANET

Yair Allouche and Michael Segal

Communication Systems Engineering Department, Ben-Gurion University of the Negev, Beer-Sheva, Israel

Phone: +972(8)6477234, Fax: +972(8)6108663, Email: segal@bgu.ac.il

Abstract In this paper we introduce the Cluster-Based Beacon Dissemination Process (CB-BDP) that aims to provide vehicles with a local vehicle proximity map of their vicinity. Based on this map, safety applications can be used for accident prevention by informing drivers about evolving hazardous situations. The CB-BDP is designed under the two following objectives. First, since it is used for safety applications, we want the map to be detailed and accurate as much as possible. Second, we want the map to be coordinated with nearby vehicles, thereby allowing synchronized and coordinated reactions of nearby vehicles to evolving hazardous situations. We design a cluster based aggregation-dissemination beaconing process that uses an optimized topology to distribute the vehicle proximity map. The topology is adaptive and robust in order to meet the challenging VANET conditions. An accurate and detailed map results in a heavy load of beacon messages. Our proposed scheme deals with this problem by integrating a contention-free medium access control (MAC) strategy for reliable communication.

Keywords Beacon dissemination · distributed algorithm · medium access control · self-organizing topology

1 Introduction

Vehicular ad hoc network (VANET) is a promising branch of traditional MANET. VANET is designed to provide wireless communication between vehicles and between vehicles and nearby roadside equipment. This communication intends to improve both safety and comfort on the road. The majority of VANET applications require the availability of real-time position information. Some of VANET applications, such as Adaptive Cruise Control and Cooperative Intersection Safety, require a certain degree of positioning accuracy in order to be able to function properly. For new research tendencies and state of the art of VANETs see [37-39]. Critical safety applications though, such as the Vehicle Collision Warning and the Cooperative Awareness applications, which enhance the driver's perception and knowledge of the road and the environment, require very precise and reliable localization system. The acceptable localization error in these applications is with a meter in order to estimate accurately

the distances between vehicles and between vehicles and objects.

The US FCC has allocated 75 MHz of the spectrum in the 5.9 GHz band for Direct Short Range Communication (DSRC). The DSRC spectrum is divided into seven 10 MHz channels. One of these seven channels is designated as a control channel, and is used primarily for safety related applications. There are two types of traffic safety-related communication that circulate on the control channel: the event-driven messages that are sent whenever a hazard situation has been detected and the periodic beacon messages by which vehicles announce their current status information – such as position, speed, steering – to nearby vehicles. Those beacon messages are a key component of safety applications by providing vehicles with a broad and accurate *vehicle proximity map* [1,2] of their surroundings. Based on this map, safety applications – usually referred to as Cooperative Awareness applications – can be used for accident prevention by informing drivers about evolving hazardous situations.

The dissemination processes of event-driven messages and beacon messages have distinct objectives and characteristics. Event-driven messages on the one hand are triggered only at detection of an emergency situation, and therefore, are not expected to cause significant load on the channel. However, once a hazardous situation is detected, an emergency message must be distributed in the complete *dissemination area* with high reliability and short delay. Beacon messages on the other hand have a more relaxed deadline requirement, but are expected to cause the significant load on the channel.

In this paper we introduce the Cluster-Based Beacon Dissemination Process (CB-BDP). This process aims to provide vehicles with such *vehicle proximity map* of their vicinity. The CB-BDP is designed with two objectives in mind. First, since the vehicle proximity map is used for safety applications, we want the map to be broad and as accurate as possible. Second, we want the map to be coordinated with vehicles located nearby. This coordination is required for the synchronized and cooperative reaction of nearby vehicles to evolving hazardous situations. However, such an accurate

estimation in a dynamic environment requires a high transmission frequency of beacon messages from numerous nearby vehicles, which in turn, results in a high data load on the channel. Moreover, coordinating a map in a lossy channel is challenging because proximity information may be received by some vehicles and not received by others.

To address these challenges, we suggest replacing the traditional multipoint to multipoint transmissions of beacon messages with a cluster-based aggregation-dissemination process. In this way, nearby vehicles share a coordinated map of their vicinity. To deal with the high load of beacon messages, we introduce a contention-free Medium Access Control (MAC) scheme intended to grant the CB-BDP with efficient and reliable spatial bandwidth reuse.

The first step to achieve this goal is to integrate cluster-based MAC [3,4] into our scheme. In cluster-based MAC, the channel access of cluster members is synchronized in order to provide contention-free channel access within the cluster. Furthermore, cluster-based MAC can provide bandwidth efficiency by bandwidth reuse among clusters. However, for reliable bandwidth reuse the resulting inter-cluster interference needs to be reduced.

In order to deal with this inter-cluster interference, we propose to combine cluster-based MAC with inter-cluster colouring scheme used to synchronize channel access between adjacent clusters. The cluster colouring is used by the CB-BDP to mitigate the inter-cluster interference by providing two levels of bandwidth reuse. The first level is a complete inter-cluster bandwidth reuse at which bandwidth is reallocated among all clusters. The inter-cluster colouring is used to reduce the inter-cluster interference by synchronizing concurrent transmissions taking place in adjacent clusters according to a fair Signal to Interference plus Noise Ratio ($SINR$) optimization criterion. The second level is less efficient but more reliable bandwidth reuse. In this case, the cluster colouring enables highly reliable transmission by silencing not only transmitter cluster members but also members of the two adjacent clusters.

This paper is organized as follows. In Section 2 we present related work. The system model is described in Section 3. In Section 4 we present the Cluster-Based Beacon Dissemination Process. Section 5 illustrates simulation results of CB-BDP. Discussion (incorporating RSUs) and conclusions are provided in Sections 6 and 7.

2 Related work

The IEEE 802.11p standard, designed for wireless access in the vehicular environment (WAVE) uses the CSMA/CA as its MAC method, despite the fact that it is suffering

from the following well-known problems. First, when considering broadcast transmission, RTS (Request To Send)/CTS (Clear To Send) mechanism is infeasible. In such case, the CSMA provides no means to solve the hidden station problem, which in a heavy traffic load can lead to a high rate of packet collisions. Second, the CSMA can lead, under high traffic load, to unacceptable channel access delays, and therefore is unable to support real-time communications.

Recent studies have demonstrated that under congested network scenarios the performance of IEEE 802.11p deteriorates significantly, resulting in unreliable communications [3,5,6]. In [3] the authors show that even in an average density of 8 vehicles per kilometre existed, only 10% of the data is transmitted without collisions. In [6] the authors show that a specific vehicle is forced to drop over 80% of its beacon messages because no channel access was possible before the next message was generated. These results imply that in congested network scenarios the IEEE 802.11p may be insufficient to provide the reliable and real time communication required by cooperative awareness safety applications. Thus, there has been extensive research to study and improve the performance of IEEE 802.11p in congested scenarios. The focus has been on controlling the message transmit rate, such as [7,8], or transmit power, such as [9], while others focused on adjusting the contention window size [10] or the carrier sensing threshold [11]. In [12], the authors survey existing adaptive beaconing approaches including adaptive beacon transmission power, beacon rate adaptation, contention window size adjustment and hybrid adaptation beaconing techniques.

A different MAC approach suggested for VANET (e.g, [13-15]) is to use channelization-based MAC scheme (as TDMA) rather than the current CSMA/CA contention-based approach. The main objective in these works is to support real time deadlines. The Space Division Multiple Access (SDMA) [13] scheme defines a one-to-one map between the space divisions and the bandwidth divisions, so within each bandwidth division a TDMA scheme is mapped. This scheme provides users with collision-free access to the communication medium, and guarantees delay-bounded communication in real-time. However, this mapping is likely to be impractical in a real system [16], mainly because of the lack of flexible adaptation to the scalable and dynamic vehicular environment. Another TDMA approach is the Self-organizing Time Division Multiple Access (STDMA) [14]. The STDMA algorithm is found in a standard for the shipping industry, automatic identification system. In this scheme each node is engaged to a slot within the frame. During the initialization, the node will listen for the channel activity during one frame and then will pick a slot randomly within the frame that is

not currently occupied by someone else. If all slots within the frame are occupied, the slot used by a station located furthest away from oneself will be chosen.

In this paper we present a different approach which is cluster-based MAC scheme [3,4, 17,18,19] in order to deal with congested network scenarios. In what follows, we describe in more details the most relevant cluster-based MAC schemes in the literature. In [17], Bononi and Felice propose a cross-layered MAC and clustering solution for supporting the fast propagation of broadcast messages in a vehicular environment. A distributed, proactive dynamic clustering algorithm is proposed to create a dynamic virtual backbone in the vehicular network. The vehicle members of the backbone are responsible for implementing efficient message propagation. Fast multi-hop propagation is achieved as the next hop in the backbone forwards the message immediately without releasing the channel. As a result, the medium control is inherited and propagated over pre-defined multi-hop nodes, without introducing back-off delays, as long as the multi-hop backbone is connected and no collisions occur. The main objective of this topology is fast propagation of safety messages, and thus, it may serve as the infrastructure for event-driven dissemination. However, it is inappropriate for the multipoint to multipoint and high frequency transmissions of beacon messages. In [18], Almalag et. al. [18] propose a new TDMA cluster-based MAC for intra-cluster communications design to allow vehicles to send and receive non-safety messages without falling the reliability of sending and receiving safety messages. In [19], the authors present an RSU centric cluster based MAC. In this protocol, the RSU region is divided into prefixed clusters. In order to increase bandwidth availability, frequency reuse in non adjacent clusters is applied. Results show that the protocol has high throughput even for high data traffic load.

In [3], Günter et al. present a medium access mechanism in which the clusterhead is responsible for assigning bandwidth to the nodes in its cluster according to the specific protocol requirement. The clustering scheme is based on a heuristic strategy in which vehicles distribute their state by the regular transmission of beacons. Each vehicle chooses its appropriate state, according to the state of the vehicles nearby. This clustering strategy produces overlapping clusters where vehicles in the overlapping sections (i.e., vehicles located within the transmission range of more than one clusterhead) act as gateways. In this way, clusterheads can communicate via two-hop links. However, as it highlight in the simulation results, the overlapping clusters result in high inter-cluster interference.

Su and Zhang [4] propose a cluster-based multichannel communications scheme that supports both public safety message delivery and infotainment applications. Each vehicle is equipped with two sets of transceivers. In each clusterhead, one transceiver uses contention-free TDMA-based MAC over the first transceivers, which are used to collect and deliver safety messages and control packets within this cluster. The second transceiver is used to exchange safety messages among clusterheads through contention-based MAC. In each cluster member, one transceiver is dedicated to communicating with the clusterhead and the other transceiver can be used to transmit the non-real-time traffic. To let two nearby neighbouring clusterheads communicate in one hop, the authors suggest limiting the intra-cluster transmission range by at least half of the inter-cluster transmission range. To reduce interference from neighboring clusters, different clusters are assigned different code-division multiple access (CDMA) codes. When a vehicle decides to become a clusterhead, it chooses randomly from a list of CDMA codes and informs its cluster members about it. Though this strategy addresses the inter-cluster interference, it results in inefficient bandwidth reuse among clusters. In this paper we will demonstrate that our CB-BDP applies *efficient* and *reliable* bandwidth reuse.

3 System Model

In this work we consider a distributed beacon dissemination process based on Vehicle to Vehicle (V2V) communication in changing dynamic environments such as highway and suburban scenarios. Accordingly, we leave the discussion about beaconing process around intersection junction out of the scope of this paper. This is because beaconing process on intersection is distinctive in terms of both objectives and challenges. On intersection, RSUs will be deployed in order to enable safe traffic merging from the different intersecting roads (e.g., the safety application Blind Merge Warning¹). This implies that on intersection the main safety messages exchange will be between vehicles and the nearby RSUs. For such traffic, a channelized cluster based MAC is preferable since it can provide high bandwidth efficiency and channel access prioritization (e.g., according to the distance to the intersection). We will discuss how our solution can be integrated with such channelized cluster based MAC in Section 6, noticing that the detailed analysis of this mechanism is out of scope of this paper.

In addition, vehicles are assumed to travel in the same direction along a road with a single entrance and exit. This

¹ This application warns a vehicle whether it is attempting to merge from a location with limited visibility having another approaching vehicle be predicted to occupy the intended merging space.

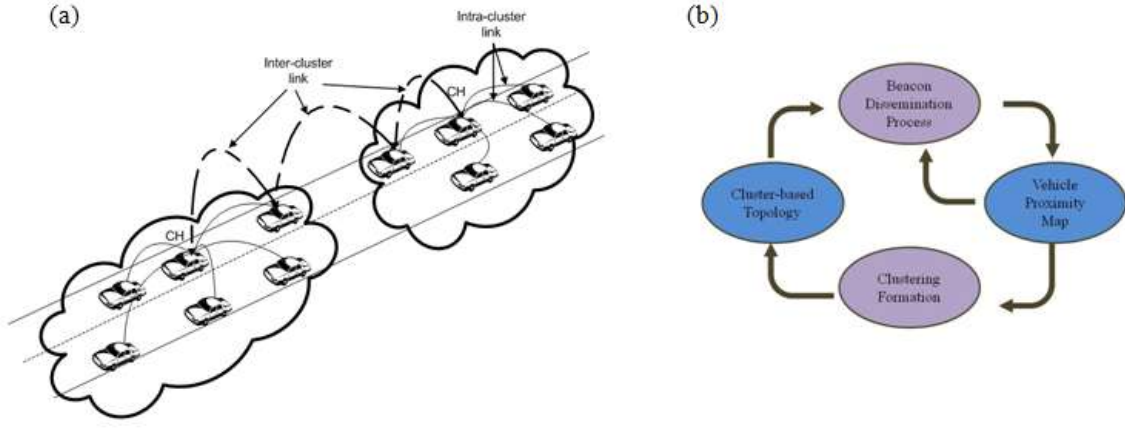


Fig. 1. (a) The cluster-based topology used by the CB-BDP. This topology is created by grouping sets of sequential vehicles into clusters. At the intra-cluster level, the members of each cluster are linked to a designated clusterhead (CH). At the inter-cluster level, clusterheads are connected via multi-hop link. (b) The interaction of D-CUT algorithm and CB-BDP .

assumption is viable as vehicles travelling in the same direction share similar moving patterns due to traffic laws and road structures, thereby creating a stable topology.

The CB-BDP manages the channel access for each road segment separately. Thus, when different road segments interfere with each other (e.g., when the vehicles travelling in opposite directions are interfering with each other) we assume that the different road segments are assigned orthogonal channel resources.

In the following section we present the clustering formation strategy used by the CB-BDP and the way the D-CUT algorithm and the CB-BDP interact.

3.1 Clustering Formation

The CB-BDP exploits cluster based topology (see Fig. 1(a)) to be the infrastructure for its beaconing process. Each cluster contains a designated vehicle referred to as the *clusterhead*, connected by one-hop *intra-cluster links* to its cluster members. The second level of the topology consists of multi-hop, *inter-cluster links* that connect adjacent clusterheads.

In [20], we introduced the D-CUT algorithm. The D-CUT algorithm is an iterative algorithm, which strives to discover and maintain a geographically optimal clustering for the current network configuration. The D-CUT algorithm is designed specifically to enable extensive but reliable inter-cluster bandwidth reuse. Thus, the D-CUT algorithm performs with the following objectives: 1) the algorithm seeks to minimize the inter-cluster interference by producing clusters that are separated by the maximal possible inter-cluster gaps and 2) the algorithm limits cluster size in order to guarantee that each vehicle has access to a contention-free channel on which to send its message. Once limited, the algorithm aims to increase the

cluster up to its maximal size, thereby allowing the most efficient utilization of the allocated bandwidth.

In [20] we also present theoretically provable bounds for algorithm performance and a simulation study to demonstrate the ability of the D-CUT algorithm to self-start and self-maintain the geographically optimized topology under the dynamic nature of VANET environments. Specifically, we demonstrate the convergence of our algorithm to a solution which meets objective 1 and approximates objective 2 by a factor smaller than 3. We demonstrate that the convergence process requires $O(\Delta)$ worst case time; and $O(\log \Delta)$ expected time where Δ indicates the distance between the initial solution and the optimal solution.

The D-CUT algorithm and the CB-BDP interact in the following way (see Fig. 1(b)). Every predefined ρ number of CB-BDP iterations, the D-CUT algorithm gets the current snapshot of the local vehicle proximity map from the CB-BDP and updates the clustering solution according to the recent changes in the network configuration. Due to the dynamic nature of the VANET environment, a feasible communication protocol for VANETs must be based on local information. Hence, the D-CUT algorithm is based on the proximity map of each vehicle's cluster and that of its two adjacent clusters. The CB-BDP uses the topology updated by the D-CUT algorithm for the next ρ CB-BDP iterations.

4 The Cluster-Based Beacon Dissemination Process

The Cluster-Based Beacon Dissemination Process (CB-BDP) is designed to provide vehicles with a broad, accurate, and coordinated vehicle proximity map of their vicinity. To achieve this, the CB-BDP applies the following three-phase process. In the first phase, beacons in the same cluster are aggregated by clusterheads using

the intra-cluster aggregation protocol. The key objective of this protocol is to provide each cluster member with access to a time bounded, contention-free channel on which to send its message. In the second phase, adjacent clusterheads exchange their cluster status using the multi-hop inter-cluster communication protocol. In the final phase, using the intra-cluster dissemination protocol, clusterheads broadcast the aggregated information to all their cluster members, providing each cluster member with a local vehicle proximity map. As the map is broadcasted from a single source, each cluster member successfully receiving this broadcast transmission obtains the same vehicle proximity map of its surroundings.

In order to attain reliability under the high data load of beacon transmissions, the above three protocols use contention-free MAC that combines intra-cluster and inter-cluster channel synchronization. The intra-cluster aggregation protocol provides high bandwidth efficiency to the beacon dissemination process by applying extensive inter-cluster bandwidth reuse. That is, the aggregation process takes place simultaneously in all clusters. This efficient bandwidth reuse in the aggregation phase makes the channel available for more reliable map dissemination and the adjacent clusterheads' communication. Specifically, we use cluster colouring to attain highly reliable transmission by silencing not only the transmitter's cluster members (as in cluster-based MAC) but also members of the two adjacent clusters.

The rest of this section is organized as follows. First, we describe the different types of messages used by the CB-BDP. Then, we present a cluster colouring scheme used to synchronize the channel access between adjacent clusters. Following this, we present the three communication protocols used by the CB_BDP to form and disseminate the vehicle proximity map. Then, we analyze the time allocation required by the CB-BDP. Finally, we present a context adaptive beacon transmission rate scheme that utilizes the coordinated vehicle proximity map in order to adapt vehicles' beacon transmission rates according to vehicle behaviour and the road conditions in which they are situated.

4.1.1 CB-BDP message types

The CB-BDP uses three message types (see Table 1): the cluster members' beacon messages, which are aggregated by clusterheads, the cluster status messages exchanged by two adjacent clusterheads, and the local vehicle proximity map messages disseminated by clusterheads in the final phase. The beacon messages contain the current status information – such as position, speed, steering – of the cluster members. In order to obtain a secure beaconing process [20], beacon messages are signed and carry a certificate to confirm valid network participants.

Table 1 –The different types of messages used by the CB-BDP. (a) presents the beacon messages of cluster member $u_{i,j}$, (b) presents C_i 's cluster status message with two options for the security header and (c) presents the vehicle proximity map message of the cluster C_i . The output of the function $\Gamma(m)$ is the compressed information of m .

(a) Cluster member beacon message($u_{i,j}$)		
Header	Payload($u_{i,j}$)	Security Header($u_{i,j}$)
	<i>posision, speed, steering..</i>	$\{Sig(u_{i,j}), Cert(u_{i,j})\}$
(b) Cluster status message (C_i)		
Header	Payload(C_i)	Security Header(C_i)
	$\Gamma\{\cup Payload(u_{i,j})\}$ $u_{i,j} \in C_i$	<u>Option 1:</u> \cup Security Header($u_{i,j}$) $u_{i,j} \in C_i$
		<u>Option 2:</u> $\{Sig(ch_i), Cert(ch_i)\}$
(c) Vehicle proximity map (C_i)		
Header	Payload(C_i map)	Security Header(C_i map)
	$\Gamma\{\cup Payload(C)\}$ $C \in \{C_{i-1}, C_i, C_{i+1}\}$	\cup Security Header(C) $C \in \{C_{i-1}, C_i, C_{i+1}\}$

For producing the cluster status, each clusterhead applies the following three operations on the data aggregated from its cluster members. First, for better data correctness, clusterheads can crosscheck the aggregated information for consistency verification and drop or correct inconsistent messages (for more details see [21,22]). Then, clusterheads compress the aggregated information by taking advantage of the high information dependency. Finally, clusterheads attach the security header. We consider two types of security header to be attached to the cluster status. In the first, the security header contains the signatures and certificate of all cluster members' beacon messages. In the second, the cluster status will be first signed by the clusterhead and carry its certificate. Then, when the cluster status is propagated toward the adjacent clusters, the cluster status will contain message forwarder's signature and certificate. As we will demonstrate below, the latter strategy results in significant security overhead reduction. It comes with a price though, enabling clusterheads or message forwarders to inject false information within the cluster status. We will discuss this issue in section 7. Finally, the local vehicle proximity map message disseminated by clusterhead will contain the cluster status of three clusters: its own cluster and its two adjacent clusters (clusterheads can further compress the aggregated information). The security header of the three clusters is attached to the vehicle proximity map message.

4.2 Cluster colouring

In order to synchronize the channel access between adjacent clusters, it is enough to colour them with two colours. Notice that as we consider one road model, the colouring needs to be done on a chain of clusters.

Therefore, the two colouring solution exists. However, such colouring requires global information knowledge, and thus is not applicable for our case. Hence, we aim for a three colour solution (using colours R , G , and B) under two objectives: (i) minimizing communication overhead and (ii) minimizing the number of clusters coloured by the third colour, B . (The incentive for the second objective is clarified in the next subsection.)

The super-cluster structure is self-started and self-maintained in the following way. The structure is based solely on the awareness of the super-cluster endpoints of their role. At the end of the first D-CUT iteration, a random strategy is applied to initiate the structure. First, a clusterhead that is disconnected from its right neighbour cluster becomes a right endpoint of a super-cluster; a clusterhead that is disconnected from its left neighbour cluster becomes a left endpoint of adjacent super-cluster. Each of the remaining clusterheads randomly selects a number between 0 and 1. If the selected number is above a predefined threshold, the clusterhead becomes a left endpoint candidate and notifies its right neighbour clusterhead about it. A left endpoint candidate becomes a left endpoint only if its left neighbour clusterhead is not a

Clustering reorganizations may also cause variation in the super-cluster size. The free parameters l_{min} and l_{max} are used to balance the propagation delay and the number of super-clusters in the network. Divide procedure is applied when the super-cluster size is above l_{max} and Union procedure is applied when the size is lower than l_{min} . By receiving the propagation process from both sides, the cluster knows its super-cluster size. On the Divide procedure of super-cluster S , the median clusterhead and its right neighbour clusterhead become a right endpoint and a left endpoint, respectively, of two new obtained super-clusters. On Union procedure of two super-clusters S' and S'' , the left super-cluster endpoint of S'' , and its left neighbour clusterhead (which acts as the right endpoint of the adjacent super-cluster S') terminate their roles as super-cluster endpoints.

4.3.1 The Intra-cluster Aggregation Protocol

As mentioned, this protocol provides the CB-BDP its

Fig. 2. Colouring based on super-cluster structure.

a fair *SINR* optimization criterion. Broadly speaking, the protocol coordinates the channel access between adjacent clusters by taking advantage of the strong links between the vehicles located next to clusterheads to deal with the weak links of the vehicles located far from the clusterheads. In addition, a power assignment scheme is applied to fairly equalize the joint interference of the concurrent transmissions.

Next, we describe our general scheduling and power allocation problem. We are given a set of clusters $\{C_1, C_2, \dots, C_n\}$ along a road in which each cluster C_i contains a clusterhead ch_i and a set of cluster members $\{u_{i,1}, u_{i,2}, \dots, u_{i,k}\}$, where $k \leq k_{max}$. Our goal is to assign each cluster member with a time slot and transmission power so the minimal *SINR* is maximized, where the *SINR* of the vehicle $u_{i,m} \in C_i$ is defined by:

$$SINR(u_{i,m}) = \frac{P_r(u_{i,m})}{\sum_{u_{j,*} \in I(u_{i,m})} P_r(u_{j,*}) \cdot G_i(u_{j,*}) + n_0}, \quad (1)$$

where $P_r(u_{i,*})$ is the received power of the link $u_{i,*}$ to ch_i , n_0 is the background noise, $I(u_{i,m})$ is the set of members from other clusters that transmit in the same time slot as $u_{i,m}$, and $G_i(u_{j,*})$ is the ratio between the received power at ch_i and ch_j during the transmission of $u_{i,*}$. Below, we will refer to $G_i(u_{j,*})$ as the *crosstalk coefficient* of the cluster member $u_{i,*}$ on C_i .

A longstanding result of the power-control theory is that maximizing the minimum *SINR* is achieved by balancing the *SINRs* of all concurrent transmissions on a common maximum level [23, 24]. This common maximum level is the outcome of the set of intra-cluster links scheduled in the same time slots. Since our objective is a solution that is based on local information, global balancing is infeasible. Next, we aim to leverage the special characteristics of our model in order to approximate this global balancing.

For this purpose, we subdivide the inter-cluster potential interferers into *primary* and *secondary* interferers. We define the vehicles in the two immediate sub-clusters as primary interferers and the rest as secondary (cluster division into two sub-clusters is based on clusterhead location).

In order to understand the rationale behind this subdivision, Fig. 3 presents a typical example of crosstalk coefficient $G_i(u_{j,*})$ behaviour as a function of the distance to ch_i (based on the two ray ground propagation model [25]). This crosstalk coefficient presents the ratio between the signal level of a link in cluster C_j and the resulting interference on the simultaneous link in cluster C_i . Thus, it signifies the impact of the scheduling and power allocation strategies of cluster C_j on cluster C_i . When studying the crosstalk coefficient as a function of the distance to ch_i ,

one can observe that the crosstalk coefficient $G_i(u_{j,*})$ exponentially decreases in accordance to the distance to ch_i and exponentially increases in accordance to the distance to ch_j . Specifically, consider the case where $j = i+1$ and $u_{j,*}$ is located exactly between ch_i and ch_{i+1} , i.e., when the distance to ch_i is 250 m. In this case, $G_i(u_{i+1,*}) = 1$. When moving $u_{i+1,*}$ toward ch_{i+1} the crosstalk coefficient decreases due to both: the distancing from ch_i and the nearing to ch_{i+1} until reaching ch_{i+1} where $G_i(u_{i+1,*}) = 0$ (at 500m). Then, when further moving $u_{i+1,*}$ the cross talk coefficient increases when distanced from ch_{i+1} but also decreases (at a lower rate) when distancing from ch_{i+1} and reaching 0.11 at 750m.

According to the above, $G_i(u_{i+1,*})$ varies in a much more significant manner in the immediate sub-cluster than in the next immediate sub-cluster. Thus, the impact of the scheduling and power allocation strategies of the primary interferers has the most influence on the interference measured at ch_i . Therefore, in order to achieve locality, we suggest scheduling and power allocation strategies that take into account only the primary interferers and consider the interference caused by the secondary interferers as a constant background noise (denoted by N).

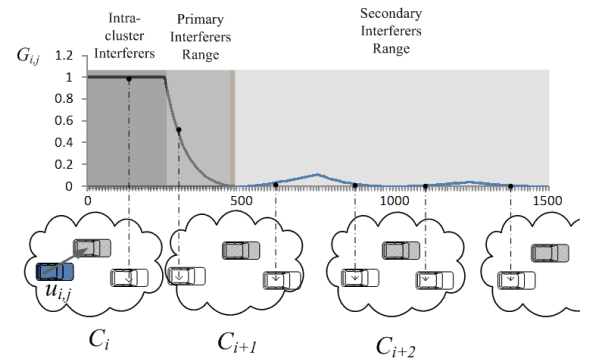


Figure 3. The crosstalk coefficient $G_i(u_{j,*})$ as a function of the distance to ch_i . The figure presents a scenario of three clusters each spread over 500 meters, and clusterheads located at the center of their clusters.

Notice that each cluster C_i consists of two sub-clusters that function as primary interferers to the two neighbouring clusters C_{i-1} , C_{i+1} . In turn, the neighbouring clusters contain two sub-clusters (the right sub-cluster of C_{i-1} and the left sub-cluster of C_{i+1}) that function as primary interferers to the cluster C_i . To obtain a local solution, we want to avoid a domino effect by primary interferers. That is, to avoid a scenario in which a number of vehicles from adjacent clusters, allocated to the same time slot, will act as primary interferers in a chain reaction. Hence, a key aspect in our solution is scheduling pairs of two sub-clusters that are the primary interferers of each other into the same time slots. To this end, we subdivide the k_{max} time slots allocated to the aggregation phase into two halves: T_I

$= \{ts_{1,1}, ts_{1,2}, \dots, ts_{1,k_{\max}/2}\}$ and $T_2 = \{ts_{2,1}, ts_{2,2}, \dots, ts_{2,k_{\max}/2}\}$. The left sub-cluster of C_i and the right sub-cluster C_{i-1} are scheduled at one half (e.g., T_1) and the right sub-cluster C_i with the left sub-cluster C_{i+1} are scheduled at the second half (e.g., T_2) of the time-slots.²

Based on this strategy, *SINR* balancing of primary interferers can be done independently and based on local information only. Consider two mutual primary interferers: $u_{i-1,x}$ and $u_{i,y}$, scheduled to the same time slot. Then, *SINR*'s balancing is achieved by balancing only their two concurrent intra-cluster links (i.e., the link between $u_{i-1,x}$ and ch_{i-1} and the link between $u_{i,y}$ and ch_i), which are given by:

$$SINR(u_{i-1,x}) = SINR(u_{i,y}), \quad (2)$$

$$\frac{p_r(u_{i-1,x})}{p_r(u_{i,y}) \cdot G_{i-1}(u_{i,y}) + N} = \frac{p_r(u_{i,y})}{p_r(u_{i-1,x}) \cdot G_i(u_{i-1,x}) + N}.$$

Based on (2), the vehicles $u_{i-1,x}$, $u_{i,y}$ can deduce the required transmission power to attain local *SINR* balancing. Additionally, given any mutual primary interferer pair, the common maximum *SINR* level of this pair can be derived from (2). Let $\beta(u_{i-1,x}, u_{i,y})$ denote the common maximum *SINR* level of the pair: $u_{i-1,x}$, $u_{i,y}$. That is,

$$\beta(u_{i-1,x}, u_{i,y}) := SINR(u_{i-1,x}) = SINR(u_{i,y}) \quad (3)$$

Next, we present a local *Max-Min SINR* scheduling that couples mutual primary interferers according to their common maximum *SINR* levels. To do this, notice that (3) can be rewritten as:

$$\beta(u_{i-1,x}, u_{i,y}) := \sqrt{\frac{p_r(u_{i-1,x})}{p_r(u_{i,y}) \cdot G_{i-1}(u_{i,y}) + N} \cdot \frac{p_r(u_{i,y})}{p_r(u_{i-1,x}) \cdot G_i(u_{i-1,x}) + N}}. \quad (4)$$

From (4) we learn that when the crosstalk-coefficient of either $u_{i-1,x}$ or $u_{i,y}$ is increasing, $\beta(u_{i-1,x}, u_{i,y})$ is decreasing. Thus, given two pairs of mutual primary interferers $\{u_{i-1,a}, u_{i,b}\}$ and $\{u_{i-1,c}, u_{i,d}\}$, such that: (i) $G_i(u_{i-1,a}) < G_i(u_{i-1,b})$ and (ii) $G_{i-1}(u_{i,c}) < G_{i-1}(u_{i,d})$, then the *Max-Min SINR* scheduling of those pairs will be achieved when each small crosstalk coefficient is coupled with the corresponding large crosstalk coefficient, i.e., when $u_{i-1,a}, u_{i,d}$ are scheduled to one time slot and $u_{i-1,b}, u_{i,c}$ are scheduled to a second time slot. To see this, notice that $\beta(u_{i-1,b}, u_{i,d})$ increases when either $G_{i-1}(u_{i,d})$ is replaced by $G_{i-1}(u_{i,c})$ or when $G_i(u_{i-1,b})$ is replaced by $G_i(u_{i-1,a})$. Thus, $\beta(u_{i-1,a}, u_{i,d})$ and $\beta(u_{i-1,b}, u_{i,c})$ are both bigger than $\beta(u_{i-1,b}, u_{i,d})$.

This observation implies that given two sets of mutual primary interferers, the following scheduling strategy

² The D-CUT algorithm can be easily modified in order to ensure that each sub-cluster size is at most $k_{\max}/2$. From the simulation results we learn that this modification is not required.

attains the local *Max-Min SINR*. We start by coupling the cluster member with the maximal crosstalk coefficient. According to the above observation, the local *Max-Min SINR* is obtained by allocating the cluster member with the maximal crosstalk-coefficient from one set in the same time slot as the cluster member with the minimal crosstalk coefficient from the second set. Following the same logic, we continue by coupling the cluster member with the next maximal crosstalk coefficient with the same time slot as the cluster member with the second minimal crosstalk coefficient. We continue with this process until we assign each cluster member of the two sets with a time slot.

According to the above, given the mutual primary interferer sub-clusters C_j^R and C_{j+1}^L , scheduled to the time slot set $T_{b \in \{1,2\}}$, where C_j^R is the right sub-cluster of C_j and C_{j+1}^L is the left sub-cluster of C_{j+1} , in the time slots $ts_{b,i}$ and

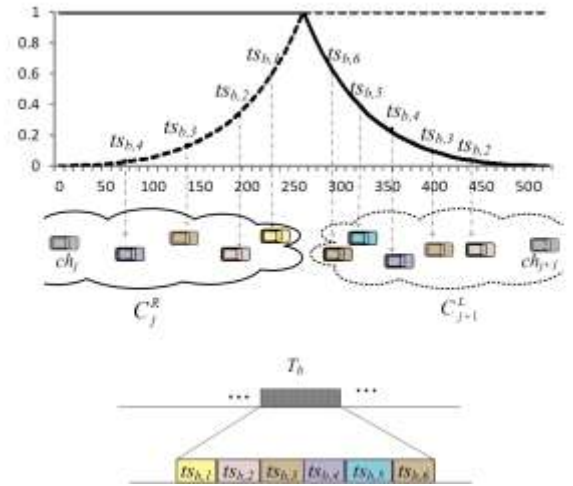


Fig. 4. The local *Max-Min SINR* scheduling strategy (for $k_{\max} = 12$). In the illustrated scenario, the member with the largest cross-talk coefficient from C_j^L and the two members with the largest cross-talk coefficient from C_{j+1}^R are assigned to the unshared time-slots: $ts_{b,1}, ts_{b,5}, ts_{b,6}$.

$ts_{b,k_{\max}/2-(i-1)}$, we allocate the vehicles with the i^{th} largest crosstalk coefficient in C_j^R and C_{j+1}^L , respectively. Notice that in this way, when the size of one of the sub-clusters is smaller than $k_{\max}/2$, the cluster members with the largest crosstalk coefficient are assigned to time slots that are unshared by primary interferers (see Fig. 4).

The cluster colouring enables the asymmetric scheduling strategy. Consider for example the case in which cluster C_j is coloured by G and its neighbours C_{j-1} and C_{j+1} are coloured by R . The mutual primary interferer sub-clusters C_{j-1}^R and C_j^L are assigned to the first half of the time slots set T_1 . Accordingly, the mutual primary interferer sub-clusters C_j^R and C_{j+1}^L are assigned to the second half of the time slots set T_2 . When cluster C_j is coloured by R and its two neighbours by G , the mirror scheduling strategy is applied (i.e., C_{j-1}^R and C_j^L are assigned to T_2 and C_j^R and

C_{j+1}^L are assigned to T_1). Based on this strategy, when adjacent clusters are coloured by R and G each cluster has one primary interferer sub-cluster at each time slot set, and thus, primary interferers can be addressed by applying the *Max-Min SINR* strategy between mutual primary interferer sub-clusters.

However, our cluster colouring scheme may produce clusters coloured by B . Let C_j be such a cluster. After the scheduling of clusters coloured by R and G , C_j has two primary interferer sub-clusters (C_{j-1}^R and C_{j+1}^L) at T_1 and none at T_2 . On the other hand, each of its two adjacent clusters, C_{j-1} and C_{j+1} , has one primary interferer sub-cluster – C_{j-2}^R and C_{j+2}^L , respectively – at T_2 . In order to cope with this case locally, we apply the *Max-Min SINR* strategy on the $k_{max}/4$ primary interferers with largest crosstalk coefficients in each sub-cluster of C_j and its two primary interferer sub-clusters C_{j-1}^R and C_{j+1}^L . To this end, the time slots set T_1 and T_2 are evenly partitioned into $\{T_{1,1}, T_{1,2}\}$ and $\{T_{2,1}, T_{2,2}\}$, respectively. Notice that cluster members with the largest crosstalk coefficients in C_{j-1}^R are scheduled to $T_{1,1}$ while the cluster members with largest crosstalk coefficients in C_{j+1}^L are scheduled to $T_{1,2}$. Thus, the $k_{max}/4$ mutual primary interferers with the largest crosstalk coefficient in C_{j-1}^R and C_j^L apply the *Max-Min SINR* strategy at $T_{1,1}$, and the $k_{max}/4$ mutual primary interferers with the largest crosstalk coefficient in C_j^R and C_{j+1}^L apply the *Max-Min SINR* strategy at $T_{1,2}$. The rest of the cluster members from C_j^L and C_j^R are scheduled to $T_{2,1}$ and $T_{2,2}$, respectively. In order to minimize the amount of this suboptimal allocation, our cluster colouring scheme aims to minimize the number of clusters coloured by B .

It is worth noticing that by holding the members' location and colour of primary interferer sub-clusters, cluster members from these sub-clusters can conclude its transmission power and time slot allocation required for producing the local *Max-Min SINR*.

4.3.2 The Inter-cluster Communication Protocol

By the inter-cluster communication protocol, adjacent

clusterheads exchange their cluster status. The protocol uses Position-Based Forwarding (PBF) [10] incorporated with inter-cluster channel synchronization to achieve reliable information exchange in this multi-hop communication. As will be specified below, the contention process prioritizes the forwarders according to their distance to the message destination. Thus, thanks to the coordinated vehicle proximity map, the contention process is coordinated among the cluster members.

In order to achieve reliability, this protocol is designed with the objective that during each transmission of the protocol the transmitter's cluster members and the members of the two adjacent clusters will all remain silent. We perform the cluster status exchange between the two adjacent clusters C_i and C_{i+1} with the corresponding clusterheads ch_i and ch_{i+1} . The protocol begins when the two clusterheads ch_i and ch_{i+1} broadcast their cluster statuses to the corresponding cluster members. Then, the cluster status message broadcasted by ch_i is delivered to ch_{i+1} by additional two-hop contention based forwarding (see Fig. 5). Specifically, we select the vehicle from C_i that is closest to ch_{i+1} and has successfully received the broadcast from ch_i as the first forwarder and the vehicle from C_{i+1} that is closest to ch_{i+1} and has successfully received the forwarding message, as the second forwarder.

Then, the cluster status message broadcasted by ch_{i+1} is delivered to ch_i by similar two-hop contention based forwarding in the opposite direction. The first forwarder is the vehicle from C_{i+1} that is closest to ch_i and has successfully received the broadcast from ch_{i+1} and the second forwarder is the vehicle from C_i that is closest to ch_i and has successfully received the forwarding message.

4.3.3 The Intra-cluster Dissemination Protocol

By the Intra-cluster dissemination protocol, a clusterhead disseminates the aggregated information to its all cluster members. Again, the D-CUT algorithm ensures that this can be done in one broadcast transmission. Again, to avoid inter-cluster interference in this central transmission, we

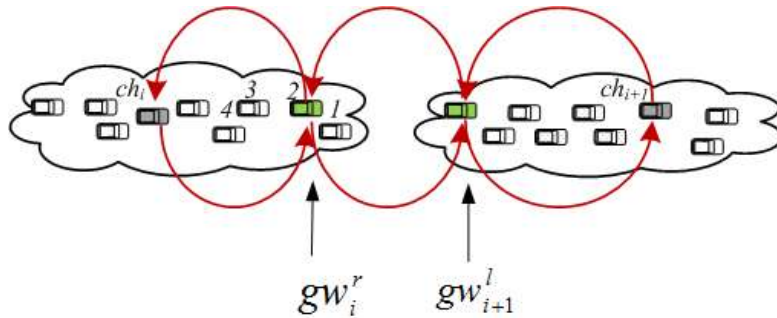


Fig. 5. Inter-cluster information exchange between the clusterheads ch_i and ch_{i+1} . The figure presents the forwarding process from ch_i to ch_{i+1} and the concurrent forwarding process from the right. As we can see, during each transmission (numbered from 1 to 3) the transmitter's cluster members and the members of the immediate adjacent cluster remain silent.

use the cluster colouring to guarantee that the two immediately adjacent cluster members will remain silent during this transmission. In this way, even the cluster members located at the edge of the cluster will be separated by at least one cluster from the closest interferer. For this purpose, the protocol allocates three time slots for the dissemination phase in which every clusterhead accesses the channel according to its cluster colour.

4.4 The CB-BDP channel allocation

The CB-BDP time allocation (see Fig. 6) consists of the time allocated to the aggregation phase T_{Agg} , the time allocated to the dissemination phase T_{Diss} , and the time allocated to the clusterhead's communication phase T_{ICC} . As mentioned above, a key design goal in our scheme is that during the aggregation phase each cluster member will receive a different time slot for sending its beacon to its clusterhead. As the D-CUT algorithm produces size-limited clusters, controlled by the algorithm free parameter k_{max} , the aggregation phase duration is given by:

$$T_{Agg} = k_{max} \cdot \left(\frac{M_1}{R_1} + T_{H,1} \right), \quad (5)$$

where M_1 and R_1 are the message size and channel rate in the aggregation phase, respectively, and $T_{H,1}$ is the time required to transmit the packet head of the message. The beacon message consists of vehicle status information and cryptographic overhead and thus can be expressed as:

$$M_1 = H_p + H_s, \quad (6)$$

where H_p is the size of payload in a cluster member beacon message and H_s is the size of the corresponding security header. The inter-cluster communication process consists of five broadcast: the initial intra-cluster dissemination and two-hop Position Based Forwarding (PBF) for each direction. The contention period is given by:

$$T_{CP} = N_p \cdot T_{slot}, \quad (7)$$

where N_p denotes the number of vehicles that participate in the forwarding contest. To address inter-cluster interference, senders from adjacent clusters are scheduled to access the channel at different time slots. This is achieved by exploiting the cluster colouring procedure, which colours the clusters in 3 colours. According to the above, the inter-cluster communication phase duration is given by:

$$T_{ICC} = N_c \cdot \left(\frac{M_2}{R_2} + T_{H,2} \right) + N_c \cdot N_h \cdot \left(T_{CP} + \frac{M_2}{R_2} + T_{H,2} \right), \quad (8)$$

where N_c is the number of cluster colours (i.e., $N_c = 3$), M_2 is the size of the cluster status message, R_2 is the channel

rate in the inter-cluster communication phase, $T_{H,3}$ is the time required to transmit the packet head of the message and N_h indicates the number of PBF transmissions in the process. In our design, $N_h = 4$. We denote the size of the compressed message m by $\eta(m)$. As the cluster size is limited by k_{max} , the maximal cluster status message size is also limited and can be expressed as:

$$M_2 = \eta(k_{max} \cdot H_p) + \lambda \cdot H_s, \quad (9)$$

where $\lambda = k_{max}$ when the security header contains the signatures and certificate of all cluster members and $\lambda = 1$ when it contains clusterhead's or forwarder's signatures and certificate. Finally, during the dissemination phase clusterheads broadcast the aggregated information in one broadcast transmission to all cluster members. Again, adjacent clusterheads are scheduled to access the channel at different time slots according to the cluster colouring. Hence, the dissemination phase duration is given by:

$$T_{Diss} = N_c \cdot \left(\frac{M_3}{R_3} + T_{H,3} \right), \quad (10)$$

where M_3 is the size of the disseminated vehicle proximity map, R_3 is the channel rate in the dissemination phase, and $T_{H,3}$ is the time required to transmit the packet head of the message. The vehicle proximity map disseminated by clusterhead contains the successfully aggregated information from its own and its two adjacent clusters. Thus, the vehicle proximity map maximal message size is given by:

$$M_3 = \eta(3 \cdot k_{max} \cdot H_p) + \lambda \cdot 3 \cdot H_s \quad (11)$$

By combining (5)-(11) we obtained that the overall time allocation required by the CB-BDP is given by:

$$T_{Total} = T_{Header} + \frac{k_{max}}{R_1} \cdot (H_p + H_s) + \frac{N_c \cdot (N_h + 1)}{R_2} \cdot (\eta(k_{max} \cdot H_p) + \lambda \cdot H_s) + \frac{N_c}{R_3} \cdot (\eta(3 \cdot k_{max} \cdot H_p) + 3 \cdot \lambda \cdot H_s) \quad (12)$$

where:

$$T_{Header} = k_{max} T_{H,1} + N_c T_{H,2} + N_c N_h (T_{CP} + T_{H,2}) + N_c T_{H,3} \quad (13)$$

Let α , $0 < \beta \leq 1$, be the portion of the bandwidth allocated to the CB-BDP (among all the traffic circulate in the channel), the CB-BDP cycle time T_{cycle} must satisfy:

$$T_{Total} \leq \beta \cdot T_{cycle} \quad (14)$$

The parameter β should be set while taking into account the different traffic that circulate in the same channel. As mentioned earlier, when different road segments interfere with each other, we assume that the different road segments are assigned with orthogonal channel resources

for conducting the CB-BDP. Furthermore, when considering the case in which emergency messages circulate in the same channel, β should be set such that

enough bandwidth is reserved to satisfy the emergency dissemination process demanding requirements.

future status. As long as a cluster member behaves “as expected” it can have unspoken understanding with its clusterhead about its status. A cluster member will inform its clusterhead about any unacceptable deviation from its expected behavior. We set vehicle proximity map accuracy criteria to define such unacceptable deviation.

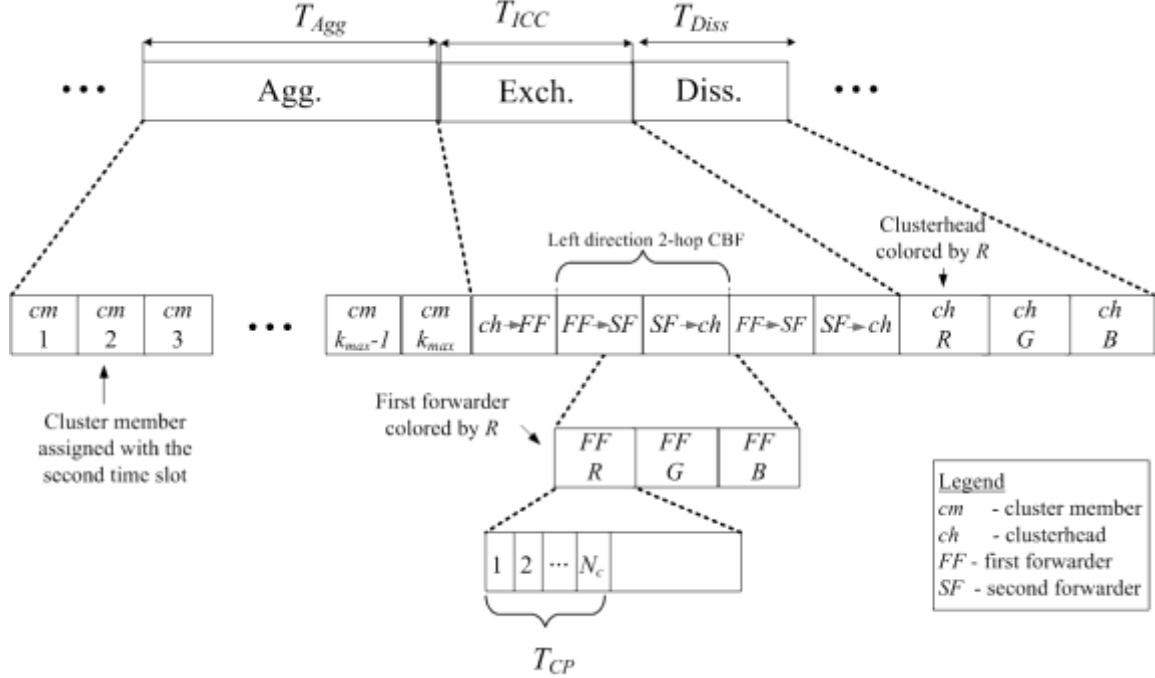


Fig. 6. The CB-BDP time table.

4.5 Context-Adaptive Beacons Transmission Rate

In this section we present a context adaptive beacon transmission rate strategy intended to reduce the load of beacon messages during the aggregation phase. The load reduction reaps two-fold benefits. First, reducing the beacon transmission rate reduces the channel load, and thus better channel performance is obtained. The second benefit is preventing clusterheads from becoming the process bottlenecks by reducing the considerable cryptographic computational overhead on their side. This overhead is due to the fact that clusterheads are required to verify the signatures and certificates of their all cluster members.

In order to reduce the load of beacon messages, we suggest leveraging on the fact that cluster members are a group of nearby vehicles constrained to similar traffic laws and road structures. Thus, by combining a traffic model (such as [26]) with the available vehicle proximity map, cluster members' behaviour is usually predictable. Broadly speaking, we suggest that clusterheads will use such a prediction model to extrapolate the cluster member's

In more detail, when a beacon message is not received by a clusterhead, the clusterhead uses an agreed prediction model to extrapolate the cluster member's future status and disseminates it in the next iteration. Thanks to the agreed prediction model and the coordinated proximity map, each cluster member can conclude its next iteration's predicted status. Thus, based on this awareness, a cluster member can deduce whether its next beacon transmission is essential to maintain the required proximity map accuracy. Accordingly, to avoid unbeneficial beacon transmission, we propose that a cluster member will send a beacon message only if its extrapolation error of its status is above some predefined threshold.

The performance of the aforementioned strategy depends on the ability of the model to predict the next status of the given vehicles. This ability depends on numerous and various factors. First, it depends on the information available for the model. Above all, whether or not the relevant roadmap is available for the model, and if it is, at what level of accuracy. Second, it depends on to what extent the traffic laws and road structures constrain vehicle behaviour. For example, it is easier to predict vehicle behaviour when it travels on a one lane road than it travels in a multilane road. Third, it depends on the ability of the

model to predict driver behaviour. For example, in the microscopic traffic model presented in [27], every vehicle has its own preferred speed, which the vehicle tries to reach if the conditions are satisfied. So assuming the driver preferred speed is available to the model, the prediction quality depends on whether the driver actually tries to reach the desired speed. In addition, vehicle status is a multidimensional parameter – such as speed, position, steering – though these parameters are highly dependent. Hence, in the following section we analyze the performance of this strategy by simulation. In this analysis, vehicles' future positions and velocities are extrapolated based on the assumption that vehicles maintain their current velocity and that the exact road structures are known.

In order to provide further insight, next we consider a simplified status extrapolation error model in order to evaluate the performance of the context-adaptive beacon rate strategy analytically. We let $\varepsilon_{i,t}$ be the status extrapolation error of vehicle i at iteration t and let Th be the maximal allowed status error. The vehicle i will transmit its beacon if $\left| \sum_{t'=t_0+1}^t \varepsilon_{i,t'} \right| > Th$ where t_0 denotes the last iteration in which a beacon message was successfully aggregated from vehicle i by its clusterhead. In other words, the disseminated map contains information about vehicle i that was last updated at t_0 .

We assume that $\varepsilon_{i,t}$ is drawn from a zero mean normal distribution with variance σ^2 , i.e., $\varepsilon_{i,t} \sim N(0, \sigma^2)$, and that the status extrapolation errors throughout the different iterations are independent. Under the above assumptions, the partial sum of the l random variables $\varepsilon_{i,t_0+1}, \varepsilon_{i,t_0+2}, \dots, \varepsilon_{i,t_0+l}$ forms a martingale. Accordingly, by the theorem of Levi [28] we obtain the expectation $E(l)$.

$$E(l) = E \left(\left| \sum_{t'=t_0+1}^{t_0+l} \varepsilon_{i,t'} \right| > Th \right) = \frac{Th^2 + Th}{\sigma}. \quad (15)$$

These results teach us that by applying our strategy, vehicles whose actions can be predicted (small standard deviation) will transmit their beacon at a low rate while vehicles that act in an unexpected manner (high standard deviation) will transmit their beacons at a high rate. The threshold Th can be used to adapt the rate according to road conditions (e.g., vehicle density).

5 Simulation

5.1 Simulation modelling and setup

The goal of this simulation study is to analyse the CB-BDP performance. We assume that all vehicles are equipped with a wireless communication device. The evaluation of the proposed CB-BDP scheme was done with a Matlab-

Table 2. Configuration setting for CB-BDP simulation study.

Parameter	Value
Frequency	5.9GHz
CB-BDP rate	5 per sec
802.11p data rate	3.6 Mbps
Background noise (n_0)	-98 dBm
Preamble length	32 μ s
PLCP header length	8 μ s
Antenna gain	2.512db
Antenna height	1.5m
Carrier wave length	50.85mm
System loss	1
Nakagami m	1,3,5
Max. Cluster size	25
Max. Trans. range	250m
D-CUT rate	1 per sec

based simulator that combines a microscopic road traffic simulation with a communication simulation.

The highway traffic model that is used in this simulation is based on the microscopic model developed by Krauss et al. [29] designed for multi-lane traffic flow dynamics. In this model, as mentioned, every vehicle has its own preferred speed, which the vehicle tries to reach if the conditions are satisfied. We set 20% of the vehicles with 25 m/s preferred speed, 50% with 35 m/s preferred speed, and 30% with 40 m/s preferred speed. In our highway traffic model, we assume that the vehicles run along a three-lane circular loop with a perimeter of 2000 m and we consider traffic densities of 18, 27, 36, 45, and 54 vehicles per km.

We assume that the contention free CB-BDP uses the DSRC's 10 MHz control channel for delivering its messages. Table 2 presents the configuration settings that have been used in this simulation study.

The packet error decision in our implementation was made probabilistically according to the Packet Error Rate methodology described in [30]. Based on the calculation of $SINR$ at each receiver, an arrived packet is determined to be successfully accepted or dropped.

The DSRC channel modelling in our simulator involves two aspects: large scale path loss and small scale fading. We use the two-ray ground model [25] for modelling the large scale path loss. The model determines the average received signal strength at a particular distance from the transmitter by considering the scenario in which there are two propagation paths between transmitter and receiver: the direct Line-Of-Sight path and a ground-reflected path.

For a more realistic propagation model, we use the probabilistic Nakagami distribution [31] to model the small scale fading phenomena existence in mobile communication channels. In the Nakagami- m model the received signal strength is derived from a multipath environment in which the different signal components

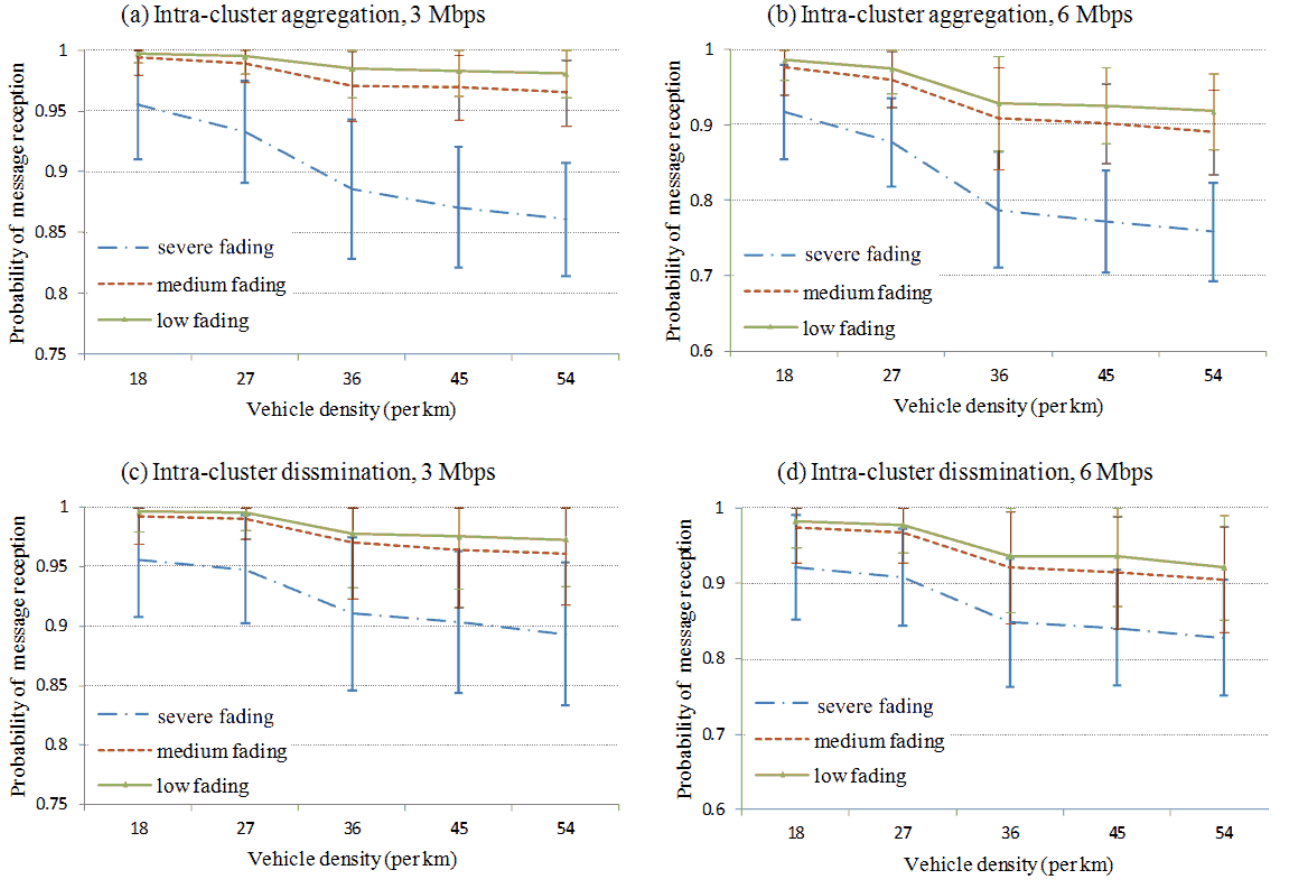


Fig. 7. The probability of successful message reception of Intra-cluster communication protocols under different fading conditions. (a,b) present the success probability of the intra-cluster aggregation protocol against vehicle density with data rates of 3 Mbps and 6 Mbps, respectively. (c,d) present the success probability of the intra-cluster dissemination protocol against vehicle density with data rates of 3 Mbps and 6 Mbps, respectively.

randomly arrive due to the different propagation phenomena. This model is widely used as a fading model wireless channel in a vehicular scenario since it has been shown to well fit empirical data (see for instance [32,33]). Inspired by [10], we evaluate the performance of our proposed scheme under three different fading intensity levels: (i) *severe fading* level in which m is configured to 1, (ii) *medium fading* level in which m is configured to 3, and (iii) *low fading* level in which m is configured to 5.

5.2 Performance evaluation

We start with studying the performance of the intra-cluster communication protocols. Fig. 7 presents the probability of successful message reception of the intra-cluster communication protocols versus vehicle density under different fading conditions. Fig. 7 (a,b) presents the success probability for the intra-cluster aggregation protocol when the data rate is set to 3 and 6 Mbps, respectively. Fig. 7 (c,d) presents the success probability for the intra-cluster dissemination protocol when data rate is set to 3 and 6 Mbps, respectively. Since the protocol performance at a given iteration largely depends on the presented road configuration, the figure also presents 95%

confidence intervals constructed across the CB-BDP iterations. From Fig. 7 we can observe that in the intra-cluster communication, the probability of successful message reception decreases slightly when vehicle density increases. This is because when density increases, the D-CUT algorithm produces clusters that are separated by smaller inter-cluster gaps, and as a result, the amount of inter-cluster interference increases. With respect to the influence of different fading conditions, we can observe that in low and medium fading conditions, even for high vehicle density, the probability of successful message reception for both protocols is above 0.95 when the data rate is set to 3 Mbps, and above 0.89 when the data rate is set to 6 Mbps. When vehicle density is set to 54 vehicles per km with medium fading conditions, 95% confidence interval is varying from 0.94 to 0.99 for the intra-cluster aggregation protocol and from 0.92 to 1 for the intra-cluster dissemination protocol. Severe fading condition causes slight performance degradation when density is low. The impact increases when the vehicle density increases. When vehicle density is set to 54 vehicles per km with severe fading conditions, the 95% confidence

interval is varying from 0.81 to 0.91 for the intra-cluster aggregation protocol and from 0.83 to 0.95 for the intra-cluster dissemination protocol. In addition, the figure shows performance degradation when switching from the 3 Mbps data rate to the 6 Mbps data rate. When vehicle density is set to 54 vehicles per km with severe fading conditions, the 95% confidence interval is varying from 0.7 to 0.82 for the intra-cluster aggregation protocol and from 0.75 to 0.9 for the intra-cluster dissemination protocol. This degradation is due to the robustness of the binary phase-shift keying (BPSK) modulation scheme, provided by the 3 Mbps data rate, compared to the quadrature phase-shift keying (QPSK) modulation scheme provided by the 6 Mbps data rate.

We continue with studying the probability of successful reception in a consecutive sequence of CB-BDP iterations in Fig. 8. This figure presents the probability of at least one successful message reception in consecutive CB-BDP iterations for the intra-cluster communication protocol when vehicle density is set to 45 vehicles per km and the data rate is set to 6 Mbps. From Fig. 8 we can observe that even under severe fading conditions, the probability of a vehicle successfully delivering its beacon message to its clusterhead in at least one of two consecutive aggregation phases is 95%. The probability of a vehicle successfully receiving the disseminated message in at least one of two consecutive dissemination phases is 96%. Due to the high rate of CB-BDP execution, the consecutive transmissions occur within a very short period of time, and thus are

changing fading conditions. Thus, repetitive transmissions even on the same link lead to such high success rates.

As mentioned, we propose two measures to allow reliable inter-cluster bandwidth reuse during the aggregation phase: the D-CUT topology optimization criteria and the channel and power allocation strategies that synchronize and equalize concurrent transmissions taking place in adjacent clusters according to a *Max-Min SINR* optimization criterion. In order to understand the contribution of our *Max-Min SINR* strategy, Fig. 9 compares this strategy with a random channel allocation strategy in which the channel is randomly allocated among the cluster members (notice that in this strategy the intra-

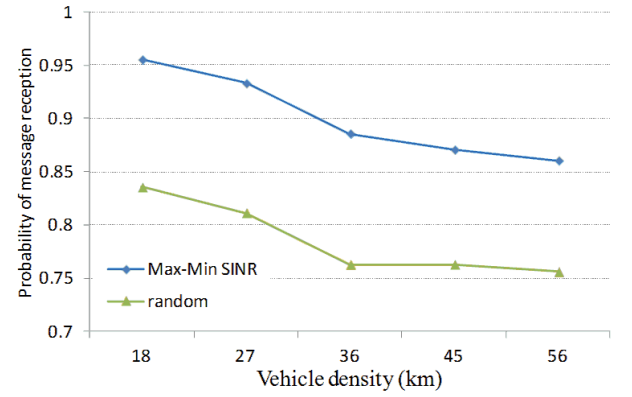


Fig. 9. A comparison between the *Max-Min SINR* and random channel access scheme in the Intra-cluster aggregation protocol with 3 Mbps data rate under severe fading level.

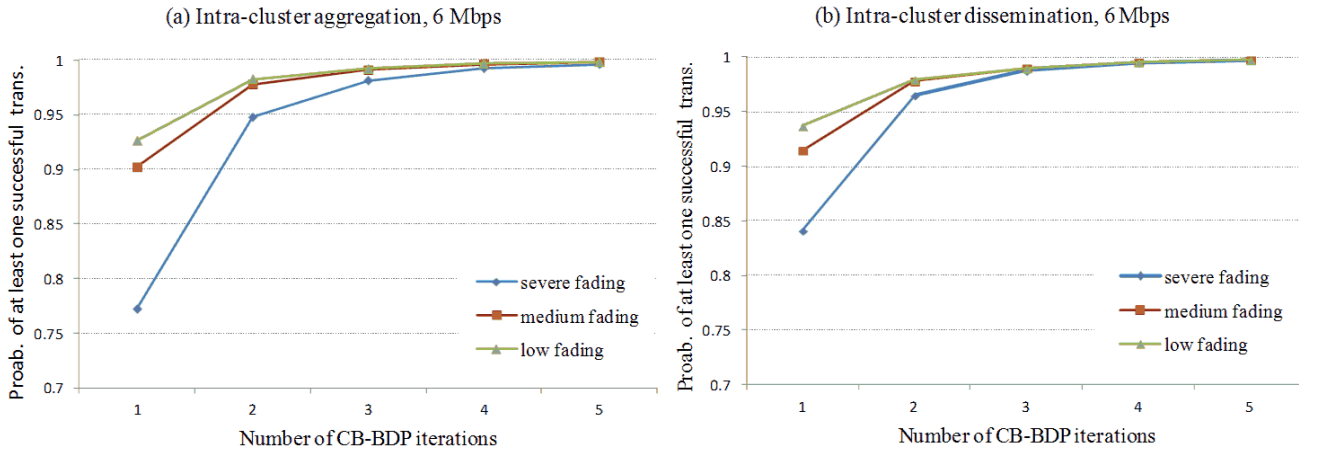


Fig. 8. The probability of at least one successful transmission in consecutive CB-BDP iterations for the Intra-cluster communication protocols. The figure presents the results for the different fading conditions while vehicle density is set to 45 vehicle per km and the data rate is set to 6 Mbps. (a) presents the probability that the same vehicle succeeded to deliver its message as a function of the number of consecutive aggregation phases. (b) presents the probability that the same vehicle succeeded to receive the broadcasted message as a function of the number of consecutive dissemination phases.

typically based on the same topology links. However, as we see from Fig. 7, performance degradation in the intra-cluster communication protocols is mainly due to fast-

cluster contention-free channel access is preserved). From Fig. 9 we can observe that our *Max-Min SINR* strategy has a significant impact on the protocol performance and leads

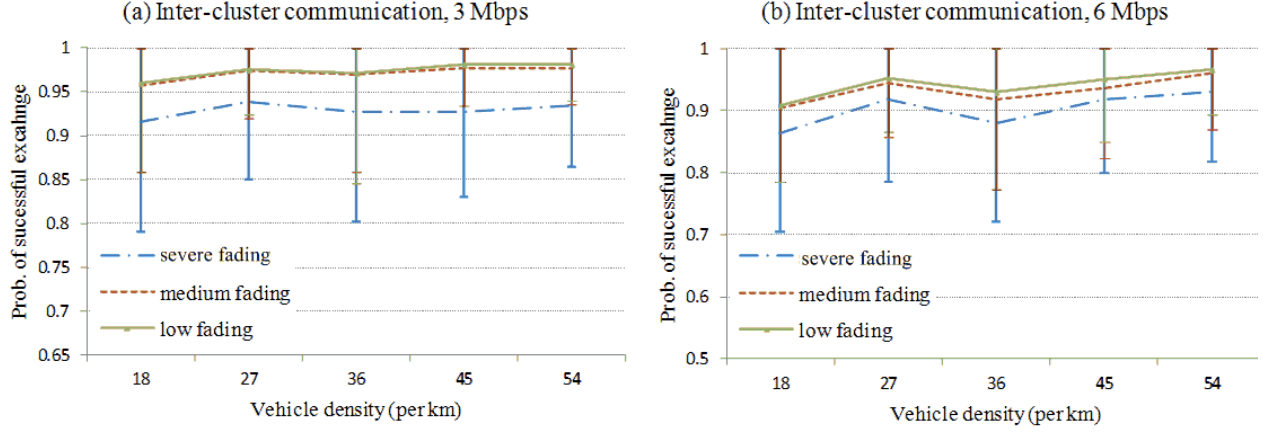


Fig. 10. The probability of successful inter-cluster communication protocol against vehicle density under different fading conditions. In (a) the data rate is configured to 3 Mbps and in (b) the data rate is configured to 6 Mbps.

to about 10% higher probability of successful message reception compared to the random strategy.

Fig. 10 presents the probability of successful inter-cluster communication protocol execution under different fading conditions, where successful protocol execution is when two adjacent clusterheads succeed in exchanging their cluster status. From this figure we can observe that the Position Based Forwarding (PBF) strategy applied by the protocol provides highly reliable information exchange even under severe fading conditions. Notice that unlike the intra-cluster communication protocols, in which success probability decreases with vehicle density, the probability of successful inter-cluster communication protocol execution fluctuates with the increase in vehicle density. This is because when vehicle density increases, the inter-cluster gaps of the D-CUT topology become smaller. Smaller inter-cluster gaps have two opposite effects on protocol execution. On the one hand, smaller inter-cluster gaps lead to higher inter-cluster interference. On the other hand, smaller inter-cluster gaps lead to information exchange between closer gateways, which increase protocol reliability. Another interesting effect is the increasing of the confidence interval range in the inter-cluster communication protocol compare to confidence interval range for the both intra-cluster communication protocols. When vehicle density is set to 54 vehicles per km, 95% confidence interval is between 0.87 and 1 for medium fading condition and is between 0.82 to 1 for severe fading condition. This can be explained by the fact that the number of clusters is significantly lower than the number of network members. Thus, the statistical population used to calculate the success probability of the inter-cluster communication protocol at each CB-BDP iteration is significantly smaller than the statistical population in the intra-cluster communication protocols.

Next, we evaluate the performance of the context-adaptive beacon rate strategy. For this evaluation, we assume that a vehicle sends a beacon message only if one of the following conditions is satisfied: (i) the difference between a vehicle's extrapolated position and its real position (determined by GPS) is above the predefined threshold Th_1 ; (ii) the differential between a vehicle's extrapolated velocity and its real velocity is above the threshold Th_2 ; and (iii) when a vehicle changes lane. We evaluate the performance for threshold: $Th_1, Th_2 \in \{2, 4, 6, 8, 10\}$ where the same threshold is used for the first two conditions, i.e., $Th_1 = Th_2$. Vehicles' future positions and velocities are extrapolated based on the assumption that vehicles maintain their current velocity and that road structures are known. Fig. 11(a) presents the effect of the context-adaptive strategy on the beacon transmission rate and Fig. 11(b) demonstrates the probability of successful message reception caused by the reduction of the beacon rate. From Fig. 11(a) we learn that even small tolerable error leads to more than 85% reduction in the beacon transmission rate. The rate further decreases when the tolerable error threshold increases. From Fig. 11(b) we can observe that reducing the beacon transmission rate during the aggregation phase reduces the inter-cluster interference, and thus, better channel performance is obtained.

6 Discussion

In this work we suggested a beaconing process designed to provide each vehicle in the network a detailed, accurate and coordinate vehicle proximity map of its surrounding area. The focus of this work is the scenario of dense network configuration expected in the late deployment phase of VANET technology. The main challenge in this scenario is addressing the high load of beacon messages required to create the desired map under the dynamic vehicular environment. In order to deal with the high data load of beacon transmissions, the CB-BDP is designed to

obtain contention-free channel access while applying efficient and reliable bandwidth reuse. To this end, the CB-BDP applies inter-cluster colouring scheme used to synchronize channel access between adjacent clusters. This enables the CB-BDP to mitigate the inter-cluster interference by providing two levels of bandwidth reuse. The first level is a complete inter-cluster bandwidth reuse at which bandwidth is reallocated among all clusters. The inter-cluster colouring is used to reduce the inter-cluster interference by synchronizing concurrent transmissions taking place in adjacent clusters according to a fair Signal to Interference plus Noise Ratio (SINR) optimization criterion. The second level is less efficient but more reliable bandwidth reuse. In this case, the cluster colouring enables highly reliable transmission by silencing not only transmitter cluster members but also members of the two adjacent clusters.

An additional key aspect of the CB-BDP is to avoid the overhead of designated control message of clustering formation and communication protocol management. This objective is achieved by letting the clustering strategy, and communication protocols to be based on the vehicle proximity map creating a reciprocal relation between the CB-BDP and the vehicle proximity map. The CB-BDP is designed to create the vehicle proximity map. The vehicle proximity map is used to optimize the topology and communication protocol in a distributed fashion.

Later, we presented the relationship between the number of the protocol's free parameters which are of significant

which the vehicle proximity map is updated. From our results we can learn that the overall time allocation required by the CB-BDP process depends mainly on four parameters: the cluster size, the channel rate, the compression function, and the security strategy. The cluster size needs to be set according to the required vehicle proximity map width as it determines the vehicles' awareness of their neighbourhood. Increasing channel rate reduces the required time allocation but also reduces the protocol performance. Since they are used for safety applications, beacon messages are usually assumed to be transmitted in low channel rate (3 Mbps or 6 Mbps) to obtain reliable communication. In our simulation study we compared the protocol performance for these two channel rate settings. Therefore, in order to allow high rate at which the vehicle proximity map is updated while maintaining communication reliability (i.e., low channel rate) and wide vehicle proximity map (i.e., a large cluster size), the main focus should be the compression function and the security strategy.

In the following we compare our scheme with related works, and describe the principles for RSUs Integration within our solution.

6.1 Time allocation comparison with the related works

As mentioned, the key objective of our scheme is to allow reliable inter-cluster bandwidth reuse during the aggregation phase. To this end, our cluster based topology is designed to minimize the inter-cluster interference by

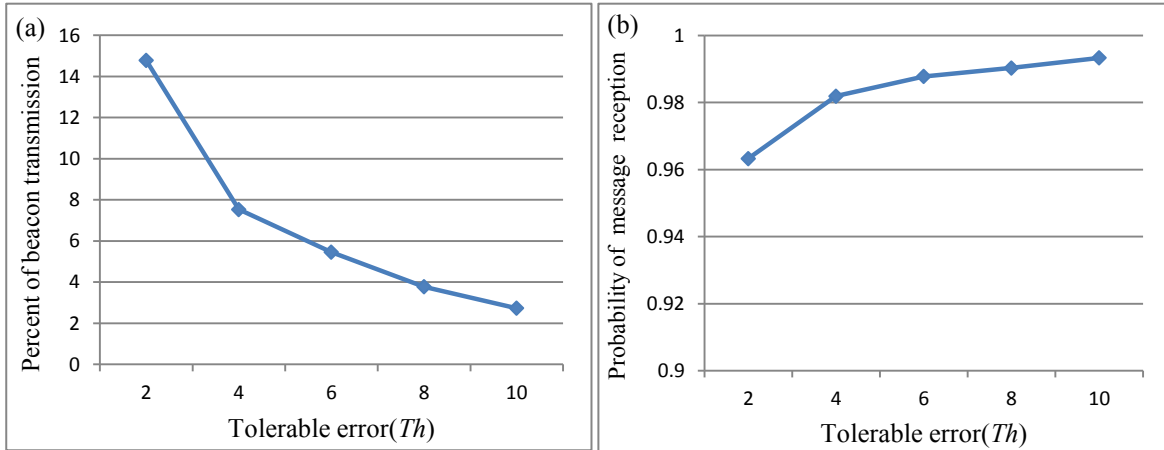


Fig. 11. Context-adaptive beacon transmission rate against the tolerable position error. The vehicle density is 45 vehicles per km, the data rate is 6 Mbps, and fading conditions are severe. (a) shows the per cent of transmitted beacons and (b) shows the effect of the context adaptive beacon rate on the probability of successful message reception during the aggregation phase.

influence on the quality of the vehicle proximity map. We derived a lower bound for the CB-BDP cycle time as function of the total time allocation required by the CB-BDP. The CB-BDP cycle time determines the rate at

producing clusters that are separated by the maximal possible inter-cluster gaps. However, this optimization results by less efficient inter-cluster communication. Specifically, in [3] the authors suggest a cluster based

topology in which clusterheads can communicate via two-hop links. However, as it highlight in the simulation results, the overlapping clusters result in high inter-cluster interference.

In the following, we compare the time allocation of our CB-BDP to a modified CB-BDP protocol that relay of a cluster based topology as in [4]. In order to resolve the high inter-cluster interference caused by the overlapping clusters, we assume that during the aggregation phase adjacent clusters are allocated with orthogonal channel resources by utilizing our inter-cluster colouring. Accordingly, in such CB-BDP the aggregation phase duration is given by:

$$T_{Agg} = N_c \cdot k_{max} \cdot \left(\frac{M_1}{R_1} + T_{H,1} \right), \quad (16)$$

The inter-cluster communication phase duration is the same as given in equation (8) but when $N_h = 3$ instead of 5. Accordingly, the CB-BDP time allocation is shorter than the modified CB-BDP if the following condition is satisfied:

$$\frac{M_2}{M_1} < \frac{k_{max}}{3}. \quad (17)$$

From equation (12) we can learn that the overall time allocation required by the CB-BDP process depends mainly on four parameters: the cluster size, the channel rate, the compression function, and the security strategy. The cluster size needs to be set according to the required vehicle proximity map width as it determines the vehicles' awareness of their neighbourhood. Increasing channel rate reduces the required time allocation but also reduces the protocol performance. Since they are used for safety applications, beacon messages are usually assumed to be transmitted in low channel rate (3 Mbps or 6 Mbps) to obtain reliable communication. In our simulation study we compare the protocol performance for these two channel rate settings. Therefore, in order to allow high rate at which the vehicle proximity map is updated while maintaining communication reliability (i.e., low channel rate) and wide vehicle proximity map (i.e., a large cluster size), the main focus should be the compression function and the security strategy.

6.1.1 Compression function

Regarding the compression function, the cluster status consists of beacon messages of nearby cluster members travelling on the same road and constrained to similar traffic law and road structure. Therefore, a high information dependency exists among the cluster members' beacon messages which can be used to obtain effective cluster status compression. In more details, the

SAE J2735 Message Set Dictionary standard [34] specifies the basic safety message (BSM) which conveys critical vehicle state information in support of V2V safety applications. A BSM must include basic information about vehicle state including vehicle's current position (in terms of latitude, longitude, and elevation), transmission speed, and brake status. In addition, BSM can also include information such as vehicle's path history and path prediction which provides a way for a vehicle to analyze the recent past and immediate future paths of neighboring vehicles. The BSM size can vary from about 40 to 150 bytes. Accordingly, a basic compression strategy for cluster status can work by representing each cluster member status relatively to some cluster reference point (e.g., representing cluster members' positions relatively to the cluster center and cluster members speed relatively to cluster members' average speed). However, since BSM mainly describes vehicle path along the road, a more sophisticated compression function can represent the road by a geometric curve (e.g., polyline) by taking into consideration the recent, current and future paths of cluster members on the road representation. Since the cluster members are travelling on the same road, this compression strategy can lead to a high compression rate. This issue is currently under our ongoing research.

6.1.2 Security overhead

A key design goal of any security mechanism is that it has a reasonable overhead. Notice that the beacon payload is usually assumed to be 150 - 200 bytes and beacon message's security header is 160 bytes [20]. Thus, we can conclude that when using the straightforward strategy in which the security header of the cluster status contains the signature and certificate of all cluster members, the security overhead is around 45% from the CB-BDP overall required time allocation when no compression is made and increases up to 60% when the compression rate is 0.5. The corresponding security overhead when the security header contains clusterhead (or message's forwarder) signature and certificate is 6% and 10%, respectively. Thus, it is preferable to apply the second strategy while providing the network with mechanisms to protect itself from false information dissemination. In [21], Raya et al. proposed a local and distributed mechanism for detection and eviction of misbehaving nodes in vehicular networks. Such mechanism can be integrated into our CB-BDP in order to protect itself from false information dissemination.

6.2 Integrating the RSUs within the topology

Extending our scheme to a full planar deployment is a subject of future research but it needs to be based on the following principles. Regarding the clustering, we assume that RSUs will act as clusterheads for a certain area around the intersection junction. Defining the boundary of the

road area only requires the RSU to notify the approaching vehicles about the RSU's cluster boundary. This simple notification mechanism ensures that the road segment is clustered independently. Notice that dynamic cluster boundary enables clusterheads to adapt their service area according to the current road density. Regarding the channel access, our inter-cluster colouring scheme, used to synchronize channel access between adjacent clusters, can be easily extended to allocate orthogonal bandwidth for the RSUs' clusters. This is because the clusters located in the boundary of the super-clusters are coloured by the colours G and R . Hence, colouring the RSUs' clusters by the colour B ensures that they are allocated with orthogonal channel resources to their adjacent clusters. The management of these orthogonal channel resources on intersection junction should be done by the RSUs in a centralized manner. Furthermore, when different road segments interfere with each other (e.g., when the vehicles travelling in opposite directions are interfering with each other) we assume that the different road segments are assigned orthogonal channel resources in order to enable independent channel access between the different sub-models. In case RSU is deployed nearby, it is its responsibility to disseminate the channel allocation between the different sub-models. Otherwise, this channel allocation requires preloading one to one mapping between sub-model and channel resource. It is noteworthy that due to the flexibility of our clustering algorithm, which produces size limited clusters, the CB-BDP channel allocation can be controlled by limiting the cluster size according to the available bandwidth.

7 Conclusions and future work

In this paper we have introduced the Cluster-Based Beacon Dissemination Process designed to provide vehicles with a real-time and coordinated *vehicle proximity map* of their vicinity. Based on this map, safety applications can be used for accident prevention by informing drivers about *evolving* hazardous situations. The real-time and coordinated map enables synchronized and coordinated reactions of nearby vehicles to the evolving situations. In [20] we proposed a clustering scheme that produces an adaptive and robust topology that is optimized specifically for an efficient and reliable beacon dissemination process. On top of this topology, we propose an aggregation-dissemination based process providing vehicles with the desired map. In order to attain reliable communication under the high data load of beacon transmissions, we propose three contention-free MAC protocols which combine intra-cluster and inter-cluster channel synchronization. The intra-cluster aggregation protocol provides high bandwidth efficiency to the beacon dissemination process by applying extensive yet reliable inter-cluster bandwidth reuse. Reliability is achieved by

synchronizing the channel access between adjacent clusters according to a fair *SINR* optimization criterion. This efficient bandwidth reuse in the aggregation phase makes the channel available for reliable intra-cluster dissemination protocols and inter-cluster communication. Based on a cluster colouring scheme, the two protocols apply less efficient but more reliable channel access; based on inter-cluster channel synchronization. The simulation results obtained show that our proposed scheme can achieve a reliable beacon dissemination process under variant highway traffic scenarios even when fading conditions are severe. In future we are planning to extend our scheme by integrating channelized cluster based MAC scheme for intersection areas. An additional interesting direction for future work is to design an hybrid channel allocation scheme in which beacon message are exchanges based on Cluster-based MAC while event driven messages are exchanged based on DSRC.

References

1. Car-2-Car Communication Consortium. (2007). Car 2 car communication consortium manifesto. Braunschweig, November.
2. Nadeem, T., Dashtinezhad, S., Liao, C., & Iftode, L. (2004). TrafficView: traffic data dissemination using car-to-car communication. In: ACM SIGMOBILE Mobile Computing and Communications Review, 8(3), 6-19.
3. Y. Gunter, B. Wiegel and H. P. Großmann (2007) Cluster-based medium access scheme for vanets. In IEEE Intelligent Transportation Systems Conference. pp. 343-348.
4. H. Su and X. Zhang (2007) Clustering-based multichannel MAC protocols for QoS provisionings over vehicular ad hoc networks. In: IEEE Transactions on Vehicular Technology, 56(6), pp. 3309-3323.
5. H. Lu and C. Poellabauer (2010) Balancing broadcast reliability and transmission range in VANETs. In: IEEE Vehicular Networking Conference (VNC), pp. 247-254.
6. K. Bilstrup, E. Uhlemann, E. G. Strom, and U. Bilstrup (2008) Evaluation of the IEEE 802.11 p MAC method for vehicle-to-vehicle communication. In: IEEE 68th Vehicular Technology Conference, pp. 1-5.
7. C.-L. Huang, Y. P. Fallah, R. Sengupta, and H. Krishnan (2011) Intervehicle transmission rate control for cooperative active safety system. In: intelligent Transportation systems, 12(3), pp. 645-658.
8. J. B. Kenney, G. Bansal, and C. E. Rohrs (2013) LIMERIC: a linear adaptive message rate algorithm for DSRC congestion control. In: IEEE Transactions on Vehicular Technology, Vol. 62, Issue 9, pp. 4182 - 4197
9. M. Torrent-Moreno, J. Mittag, P. Santi, and H. Hartenstein (2009) Vehicle-to-Vehicle Communication: Fair Transmit Power Control for Safety-Critical Information. In: IEEE Transactions on Vehicular Technology, vol. 58, pp. 3684-3703.
10. R. K. Schmidt, T. Leinmüller, and G. Schäfer, (2010) Adapting the wireless carrier sensing for VANETs. In: 6th

- International Workshop on Intelligent Transportation, Hamburg.
11. S. Rezaei, R. Sengupta, H. Krishnan, X. Guan, and P. Student (2008) Adaptive communication scheme for cooperative active safety system In: 15th World Congress on Intelligent Transport Systems and ITS America's.
 12. Kayhan Zrar Ghafoor, Jaime Lloret, Kamalrulnizam Abu Bakar, Ali Safa Sadiq, Sofian Ali Ben Mussa (2013), Beaconing Approaches in Vehicular Ad Hoc Networks: A Survey, *Wireless Personal Communications*, Vol. 73, Issue 3, pp. 885-912.
 13. S. V. Bana and P. Varaiya (2001) Space division multiple access (SDMA) for robust ad hoc vehicle communication networks. In: *IEEE Intelligent Transportation Systems, Proceedings*, pp. 962-967.
 14. Bilstrup, K., Uhlemann, E., Ström, E. G., & Bilstrup, U. (2009). On the ability of the 802.11 p MAC method and STDMA to support real-time vehicle-to-vehicle communications. In: *EURASIP Journal on Wireless Communications and Networking*. pp 1-14.
 15. H. Su and X. Zhang (2007) Clustering-based multichannel MAC protocols for QoS provisionings over vehicular ad hoc networks. In: *Veh. Technol. IEEE Trans. On*, 56(6), pp. 3309-3323.
 16. X. Chen and H. H. Refai (2008) Sdma: On the suitability for vanet. In: *Information and Communication Technologies: From Theory to Applications. 3rd International Conference on*, pp. 1-5.
 17. L. Bononi and M. Di Felice (2007) A cross layered mac and clustering scheme for efficient broadcast in vanets . In: *IEEE International Conference on Mobile Adhoc and Sensor Systems*, pp. 1-8.
 18. Chandra Rathore, N., Verma, S., & Tomar, G. S. (2010). CMAC: a cluster based MAC protocol for VANETs. In *IEEE International Conference on Computer Information Systems and Industrial Management Applications (CISIM)*, pp. 563-568.
 19. Almalag, M. S., Olariu, S., & Weigle, M. C. (2012). Tdma cluster-based mac for vanets (tc-mac). In *IEEE International Symposium on a World of Wireless, Mobile and Multimedia Networks (WoWMoM)*, pp. 1-6.
 20. P. Papadimitratos, L. Buttyan, T. Holczer, E. Schoch, J. Freudiger, M. Raya, Z. Ma. Zhendong, F. Kargl, A. Kung, J. P. Hubaux (2008) Secure vehicular communication systems: design and architecture. In: *IEEE Communications Magazine*, 46(11), pp. 100-109.
 21. Y. Allouche and M. Segal (2013) A Cluster-Based Beaconing Approach in VANET: Near Optimal Topology Via Proximity Information. *ACM Mobile Networks and Applications*, vol. 18(6), pp. 766-787.
 22. M. Raya, P. Papadimitratos, I. Aad, D. Jungels, and J.-P. Hubaux (2007) Eviction of misbehaving and faulty nodes in vehicular networks. In: *IEEE JSAC, special issue on Vehicular Networks*, 25(8), pp. 1557-1568.
 23. P. Golle, D. Greene, and J. Staddon (2004) Detecting and correcting malicious data in VANETs. In: *Proceedings of the 1st ACM international workshop on Vehicular ad hoc networks*, pp. 29-37.
 24. J. Zander and S.-L. Kim (2001) Radio Resource Management for Wireless Networks. In: Artech House, Boston, Mass, USA.
 25. H. J. Meyerhoff (1974) Method for computing the optimum power balance in multibeam satellites. In: *COMSAT Technical Review*, 4(1), pp. 139-146.
 26. T. S. Rappaport (1996) *Wireless communications, principles and practice*, section 3.6. In: Prentice Hall.
 27. G. Bansal, H. Lu, J. B. Kenney, and C. Poellabauer (2013), EMBARC: error model based adaptive rate control for vehicle-to-vehicle communications. In: *Proceeding of the tenth ACM international workshop on Vehicular inter-networking, systems, and applications*, pp. 41-50.
 28. S. Krauss, P. Wagner, and C. Gawron (1997), Metastable states in a microscopic model of traffic flow. In: *Phys. Rev. E*, vol. 55, no. 5, p. 5597.
 29. R. Durrett (2010), *Probability: theory and examples*, in: Cambridge university press, vol. 3.
 30. S. Krauss, P. Wagner, and C. Gawron (1997) Metastable states in a microscopic model of traffic flow. In: *Physical Revue*. 55(5).
 31. M. B. Pursley and D. J. Taipale (1987) Error probabilities for spread-spectrum packet radio with convolutional codes and Viterbi decoding. In: *IEEE Trans Communications*, 35(1), pp. 1-12.
 32. M. Nakagami (1960) The m-distribution: A general formula of intensity distribution of the rapid fading In: *Statistical Methods in Radio Wave Propagation*, W. C. Hoffman, Ed. Oxford, U.K.: Pergamon.
 33. J. Yin, G. Holland, T. El Batt, F. Bai, and H. Krishnan (2006) DSRC channel fading analysis from empirical measurement. In: *Proc. 1st Int. Conf. Commun. Netw. China, ChinaCom*, pp. 1-5.
 34. W. Li, H. Zhang, and T. Gulliver (2004) Error probability for maximal ratiocombining on correlated Nakagami fading channels. In: *60th IEEE VTC, Los Angeles, CA*, vol. 3, pp. 1786-1790.
 35. Society of Automotive Engineers, DSRC Committee (2009) SAE J2735 Dedicated Short Range Communications (DSRC) Message Set Dictionary, Revision 35..
 36. J. T. Isaac, S. Zeadally and J.S Camara (2010) Security attacks and solutions for vehicular ad hoc networks. In: *IET Communications*, 4(7), pp. 894 - 903.
 37. K. Z. Ghafoor, M. A. Mohammed, J. Lloret, K. A. Bakar, Zaitul M. Zainuddin (2013), *Routing Protocols in Vehicular Ad hoc Networks: Survey and Research Challenges, Network Protocols and Algorithms*, Vol 5, No 4, pp. 39-83.
 38. K. Z. Ghafoor, K. A. Bakar, Jaime Lloret, Chih-Heng Ke, Kevin C. Lee (2013), *Intelligent Beaconless Geographical Forwarding for Urban Vehicular Environments*, *Wireless Networks*, Vol. 19, Issue 3, pp. 345-362.
 39. M. Louiza, M. Samira (2013), *A New Framework for Request-driven Data Harvesting in Vehicular Sensor Networks, Network Protocols and Algorithms*, Vol 5, No 4, pp. 1-18

